PROF. KE CAO (Orcid ID : 0000-0001-5392-2306)

Article type : Original

SIRT1 regulates N^6-methyladenosine RNA modification in hepatocarcinogenesis by inducing RANBP2-dependent FTO SUMOylation

Xiaoming Liu[1,2], Jianye Liu[3], Wen Xiao[4], Qinghai Zeng[5], Hao Bo[6], Yuxing Zhu[1], Lian Gong[1], Dong He[7], Xiaowei Xing[8], Ruhong Li[9], Ming Zhou[6], Wei Xiong[6], Yanhong Zhou[6], Jianda Zhou[10], Xiaohui Li[11,12], Fei Guo[11,13], Canxia Xu[2,14], Xiong Chen[2,14], Xiaoyan Wang[2,14], Fen Wang[2,14], Qiang Wang[15], Ke Cao[1]

1. Department of Oncology, Third Xiangya Hospital of Central South University, Changsha 410013, China

2. Department of Gastroenterology, Third Xiangya Hospital of Central South University, Changsha 410013, China

3. Department of Urology, Third Xiangya Hospital of Central South University, Changsha 410013, China

4. Key Laboratory of Genomic and Precision Medicine, Collaborative Innovation Center of Genetics and Development, CAS Center for Excellence in Molecular Cell Science, Beijing Institute of Genomics, Chinese Academy of Sciences, Beijing 100101, China

5. Department of Dermatology, Third Xiangya Hospital of Central South University, Changsha 410013, China

6. Cancer Research Institute and Key Laboratory of Carcinogenesis of the Chinese Ministry of Health, Central South University, Changsha 410078, China.

7. Department of Respiratory, The Second People's Hospital of Hunan Province, Changsha 410007, China

8. Center for Medical Experiments, Third Xiangya Hospital of Central South University, Changsha 410013, China

9. Yan'an Affiliated Hospital of Kunming Medical University, Kunming 650051, China.

10. Department of Plastic Surgery, Third Xiangya Hospital of Central South University, Changsha 410013, China

11. Hunan Key Laboratory for Bioanalysis of Complex Matrix Samples, Changsha 410205, China

12. Department of Pharmaceutical Chemistry, School of Pharmaceutical Sciences, Central South University, Changsha 410013, China

13. Department of Clinical Pharmacology, Xiangya Hospital of Central South University, Changsha 410008, China.

14. Hunan Key Laboratory of Nonresolving Inflammation and Cancer, Changsha 410013, China

15. Department of Transplantation, Third Xiangya Hospital of Central South University, Changsha 410013, China

Key Words: SIRT1, m^{6}A RNA modification, FTO, SUMOylation, Hepatocellular carcinoma

Contact information

***Correspondence to**:* Ke Cao, Department of Oncology, Third Xiangya Hospital, Central South University, 138 Tongzipo Road, Changsha 410013, China

Email: csucaoke@163.com

Tel: +86 0731-88618240

Fax: +86 0731-88618285

Conflicts of interest

The authors have declared that no conflict of interest exists.

Financial support

This work was supported by the National Science Foundation of China (81874137), the Outstanding Youth Foundation of Hunan Province (2018JJ1047), the Huxiang Young Talent Project (2016RS3022), the Innovation-Driven Project of Central South University (2017CX012), and the "New Xiangya Talent Projects" of Third Xiangya Hospital of Central South University (20150201, JY201710).

List of abbreviations

HCC: Hepatocellular carcinoma

SIRT1: silent information regulator 1

m^6A: N^6-methyladenosine

FTO: fat mass and obesity-associated protein

RANBP2: RAN binding protein 2

SUMO: small ubiquitin-like modifier

GNAO1: Guanine nucleotide-binding protein G (o) subunit alpha

SILAC: stable isotope labeling with amino acids in cell culture

LC-MS/MS: liquid chromatography-tandem mass spectrometry

HPLC: high performance liquid chromatography

MeRIP-seq: methylated RNA immunoprecipitation sequencing

Summary

The deacetylase SIRT1 is crucial regulator of FTO downregulation via RANBP2-mediated SUMOylation, steering m^6A RNA modification of tumor suppressor such as GNAO1 in HCC tumorigenesis. SIRT1-derived m^6A RNA modification may offer novel therapeutic targets and strategies to treat HCC.

Abstract

***Background & Aims*:** Hepatocellular carcinoma (HCC) is associated with high malignancy rates. Recently, a known deacetylase SIRT1 is discovered in HCC, while its presence is positively correlated with malignancy and metastasis. N^6-methyladenosine (m^6A) is the most prominent modification but the exact mechanisms on how SIRT1 regulates m^6A modification to induce hepatocarcinogenesis remain unclear.

Approach & Results: Here we demonstrate that SIRT1 exerts oncogenic role by downregulating fat mass and obesity-associated protein (FTO), which is an m^6A demethylase. A crucial component of small ubiquitin-related modifiers (SUMOs) E3 ligase, RANBP2, is activated by SIRT1 and it is indispensable for FTO SUMOylation at Lysine (K)-216 site that promotes FTO degradation. Moreover, Guanine nucleotide-binding protein G (o) subunit alpha (GNAO1) is firstly identified as m^6A downstream targets of FTO and tumor suppressor in HCC, and depletion of FTO by SIRT1 improves m^6A^+ GNAO1 and downregulates its mRNA expression.

***Conclusions*:** We demonstrate an important mechanism whereby SIRT1 destabilizes FTO, steering the m^6A^+ of downstream molecules and subsequent mRNA expression in HCC tumorigenesis. Our findings uncover a novel target of SIRT1 for therapeutic agents to treat HCC.

Introduction

Hepatocellular carcinoma (HCC) is a highly aggressive cancer that has been recognized as the second leading cause of cancer-related deaths (1). Hepatocarcinogenesis is known as a complex and multimodal process experiencing genetic and epigenetic changes. Most patients are confronted with advanced diseases, but options of effective chemotherapies are limited. It is therefore urgent to understand HCC carcinogenesis at the molecular level, and to identify novel targets for developing efficacious therapeutics, thus leading to a cure of HCC.

Among different post-translational modifications (PTMs) regulatory processes, a network of reversible acetylation controls precise protein function to regulate different tumorigenesis. Alterations in an array of cellular processes driven by silent information regulator 1 (SIRT1) have been implicated in HCC tumorigenesis and progression. As a member of NAD^+-dependent sirtuin deacetylases, SIRT1 catalyzes the deacetylation of histone proteins as well as other substrates, and exerts broad effects towards inflammation, aging, calorie restriction/energetics, mitochondrial biogenesis, stress resistance, cellular senescence, endothelial functions, apoptosis/autophagy, and circadian rhythms (2, 3). It is known that SIRT1 can be oncogenic in cancers (e.g. prostate, colon, acute myeloid leukemia) and it plays a suppressing role in gastric and breast cancers (4-6). Moreover, SIRT1 overexpression is essential in the case of HCC, and its inhibition results in the impairment of tumor cell growth under *in vitro* and *in vivo* conditions (7, 8). However, up to now little is known concerning SIRT1 controlled HCC oncogenic events.

Studies have indicated that defects of RNA modification may play a role in hepatocarcinogenesis (9, 10). However, the dynamic and subtle RNA processing events underlying the effects of SIRT1 remain largely unknown. In recent year, investigations into N^6-methyladenosine (m^6A) has gathered

researchers' attention as a useful tool for mechanisms of carcinogenesis (11). It is the post-transcriptional modification that mostly occur at a subset of RRACH motifs (R = G or A; H = A, C or U), and has been identified in RNA splicing, stability, mRNA translational efficiency, secondary RNA structure, nuclear export and localization (12, 13). The dynamic of m^6A is coordinated by adenosine methyltransferases ("writers"), demethylases ("erasers"), and m^6A-binding proteins ("readers"), respectively (14). The fat mass and obesity-associated protein (FTO) plays the erasing role in the reversible methylation by m^6A both under *in vivo* and *in vitro* conditions (15). FTO is also associated with the occurrence and prognosis of tissue-specific carcinoma (16, 17). Despite the recent interest in m^6A modification, the pertinent role of m^6A and specific gene signatures related to RNA regulation by SIRT1 and FTO in the progression of HCC has not been examined previously.

In this study, E3 SUMO-ligase RANBP2 was screened and then identified as a crucial mediator of FTO downregulation by SIRT1. FTO Lysine(K)-216 was the major SUMOylation site targeted by RANBP2, and it was highly conserved among FTO orthologues in different species. Interestingly, we proved SUMO-K216 modification promoted FTO instability via potential ubiquitin pathway. Furthermore, depleted FTO by SIRT1 promoted m^6A^+ levels of HCC tumor suppressor Guanine nucleotide-binding protein G (o) subunit alpha (GNAO1) and decrease its mRNA expression. These results may introduce the novel piece to the atlas of epitranscriptomic and epigenetic regulations in SIRT1-mediated HCC tumorigenesis.

Experimental Procedures

Cell culture, Reagent and transfection

Ten HCC cell lines (Hep3B, HepG2, Huh7, SMMC-7721, BEL-7402, BEL-7404, MHCC97H, MHCC97L, MHCC-LM, and QGY7703) and one immortalized human hepatocyte (L02) were purchased from ATCC (Rockville, Maryland). The plasmids for overexpression of FTO (p3xFLAG-CMV-XN-Hfto) was a kind gift from Dr. Yungui Yang of the Chinese Academy of Sciences (Beijing, China). SIRT1-shRNA, plasmids for SIRT1 overexpression, FTO-shRNA, and RANBP2-siRNA, and GNAO1-siRNA were purchased from GeneChem Biotechnology Company (Shanghai, China). Cell culture and si/shRNA sequences were described in additional methodological details and Supplemental Table 1.

Reagents

The chemical reagents SRT2104 (SIRT1-specific agonist also known as GS2245840; cat. #s7792), Selisistat (SIRT1-specific antagonist also known as EX527; cat. #s1541), and MG132 (cat. #s2619) were from Selleckchem (Houston, TX, USA). CHX (cat. #2112s) was from cell signaling technology (Beverly, Massachusetts, USA).

Mutagenesis

Mutations and truncations of FTO were constructed by PCR-based methods in this study. FTO CDS (NM_001363894.1) was synthesized and subcloned into the vector pEGFP-C1 (Clontech, 5' BglII - 3' BamHI). In addition, Lys216 and Lys422 were mutated to arginine (R), histidine (H), and serine (S), respectively. FTO WT and mutants were validated by DNA sequencing, western blotting, and m^6A activity analyses.

Global proteome and lysine acetylation analyses

Briefly, global proteome analysis used an integrated approach involving stable isotope labeling with amino acids in cell culture (SILAC) and liquid chromatography-tandem mass spectrometry

(LC-MS/MS) to quantify the dynamic changes in the entire proteome of a cell line (the Hep3B in this case). Further, an integrated approach involving SILAC labeling, high performance liquid chromatography (HPLC) fractionation, Kac antibody affinity enrichment, and LC-MS/MS was employed to quantify the dynamic changes in the whole acetylome of the control and experimental cells. Both methods were performed with the support of PTM-Biolabs Co. Ltd. (310018; HangZhou, Zhejiang, China). See details in the supplemental information.

Western blot, Immunoprecipitation, Immunostaining, and Immunohistochemistry

The above experiments were detailed in the supplemental information with the antibodies listed (Supplemental Table 2).

Cycloheximide (CHX)-based protein stability assay

Cells were treated with 10μM Cycloheximide (CHX) for indicated periods (0h, 2h, 4h, 6h, and 12h) to block protein synthesis. 20 μM MG132 was also administrated to inhibit the proteasome before harvesting. Crude extracts were prepared, RANBP2 and FTO protein expression were then assayed as described previously (18).

RNA stability assay

To measure RNA stability, 5 g/ml Actinomycin D (Sigma aldrich, USA) was added to cells to inhibit transcription and then incubated for different time points as indicated. At each time point, RNA was harvested followed by qRT-PCR as previously described. Transcript levels were plotted by appropriate nonlinear regression curves using a one-phase decay equation. RNA decay rate constant (k) was quantified by fitting an exponential curve to the data points ($y = a*e^{-kt}$; y is the relative amount of RNA, and t is time). The turnover rate of mRNA was estimated according to previously published paper (19). The half-life was then estimated according to the equation $t_{1/2} = \ln(2)/k$. The

normalizer transcript 18S rRNA that does not decay over the course of this experiment was detected as control.

MeRIP and RNA sequencing

The control, SIRT1-overexpressing, FTO-overexpressing, and both SIRT1- and FTO-overexpressing groups were carried out in Hep3B cell line. High throughput m^{6}A sequencing and RNA array were performed under the support of Kangchen Biotech (200233; Shanghai, China). See additional methodological details.

m^{6}A dot blot

The m^{6}A dot blot assay was conducted as previously described (16). See additional methodological details.

Measurement of Total m^{6}A and m^{6}A-IP-qPCR Assay

Total m^{6}A content was measured in 200-ng aliquots of total RNA extracted from Hep3B and HepG2 cells using an m^{6}A RNA methylation quantification kit (cat. no. P-9005; Epigentek) according to the manufacturer's instructions (20, 21). MeRIP-qPCR assays were described in the additional information.

Quantitative Reverse Transcription Polymerase Chain Reaction (qRT-PCR)

See additional methodological details.

Proliferation, Apoptosis, and Invasion Assays

See additional methodological details.

Bioinformatic analyses

Protein and acetylation arrays in SIRT1-overexpressing Hep3B models were used to analyze the targets for enrichment of GO terms and KEGG pathways. The survival, differential expressing, and

correlating of the candidate gene (such as SIRT1 and GNAO1) were assessed using the Gene Expression Profiling Interactive Analysis (GEPIA) database (http://gepia.cancer-pku.cn), the starBase Pan-Cancer Analysis Platform (http://starbase.sysu.edu.cn/panCancer.php), the Cancer Genome Atlas (TCGA) database (https://cancergenome.nih.gov/), Cancer RNA-Seq Nexus (CRN) database (http://syslab4.nchu.edu.tw/), and NCBI's Gene Expression Omnibus database (https://www.ncbi.nlm.nih.gov/geo/). The GPS-SUMO (http://sumosp.biocuckoo.org/), PHYRE2 Protein Fold Recognition Server (http://www.sbg.bio.ic.ac.uk/phyre2/), and the Discovery Studio software were applied to predict the SUMO sites and functional protein-protein interactions. The m^6A binding patterns were obtained from the m^6aVar Database of functional variants (http://m6avar.renlab.org/). IGV browser software was utilized to show multiple RNA m^6A methylated sites.

Xenograft Mouse Model

In short, male BALB/c nude mice (5 weeks old) were subcutaneously inoculated in the right axillary fossa with 200 μl (1×10^6 cells) of SIRT1-overexpressing Hep3B cells, SIRT1- and FTO-overexpressing Hep3B cells, shRNA-SIRT1-transfected HepG2 cells, shRNA-SIRT1- and shRNA-FTO-transfected HepG2 cells, and control cells. Tumors volumes were calculated as described in additional methodological details and were collected for additional western blotting and immunohistochemistry.

Statistical Analysis

All experiments were performed at least in triplicate, and representative results were shown. Means, SD and SEM were analyzed using Graphpad prism 8.0. Significance tests on data sets were conducted using analysis of variance (ANOVA) followed by a comparison between the specific groups using the

Student's *t*-test. The relationship between SIRT1 expression and the clinicopathological characteristics was analyzed using the χ^2 test. In univariate survival analysis, cumulative survival curves were calculated according to the Kaplan-Meier method, and the survival curves were analyzed using the log-rank test. All analyses were conducted using SPSS (version 19.0; SPSS Inc., Chicago, IL). $^{*}P$ value < 0.05 was considered to indicate statistical significance plus $^{**}P < 0.01$ and $^{***}P < 0.001$.

Accession number

All original microarray data using liver tissues of each genotype were deposited in the NCBI's Gene Expression Omnibus database.

Study approval

All animal received human care. Human HCC specimens were collected from the Third Xiangya Hopital of Central South University between 2013 and 2017, and all of the human specimens were procured with proper written, informed consent. The study protocols conformed to the ethical guidelines of the 1975 Declaration of Helsinki and were approved by the ethics committee of Third Xiangya Hospital of Central South University.

Results

Identification of SIRT1 as biomarkers in HCC development

Three datasets downloaded from the Gene Expression Omnibus (GSE98620, GSE1898, and GSE36376) showed that SIRT1 was remarkably augmented in HCC versus normal tissue (Figure 1A). Similarly, our HCC samples had significantly increased presence of SIRT1 compared with adjacent non-neoplastic liver tissues according to the immunohistochemistry (Figure 1B) and the western blot

results (Figure 1C). The correlations between SIRT1 levels and various clinicopathological parameters were summarized in Supplemental Table 3. Chi-square analysis revealed that the level of SIRT1 in HCC tissues was highly correlated with tumor grade (Edmondson-Steiner grade, $P = 0.003$), T classification ($P = 0.013$), and N classification ($P = 0.033$). Relatively low and high endogenous SIRT1 expression was detected in Hep3B and HepG2 cells examined, respectively. Therefore, these two cell lines were considered as ideal for exploring the biological features of SIRT1 (Figure 1D). According to the results of the CCK-8 assays, SIRT1 overexpression in Hep3B cells was associated with increased proliferation, while its knockdown reduced HepG2 cell proliferation (Figure 1E, SIRT1 overexpression and knockdown verifications were shown in Supplemental Figure 1).

The deacetylase SIRT1 was therefore identified to promote HCC tumorigenesis, and its potential targets were next performed using protein and acetylation arrays. Proteome analysis of Hep3B cells indicated that 202 proteins was significantly upregulated and the expression of 252 proteins was significantly downregulated (above 1.5- or below 0.667-fold change). Next, quantitative lysine acetylome analysis showed that 209 lysine acetylation sites in 157 proteins were upregulated and 290 lysing acetylation sites in 204 proteins were downregulated (above 1.5- or below 0.667-fold change, representative heatmap in Figure 1F).

SIRT1 drives HCC tumorigenesis in an FTO-dependent manner

To better understand the role of SIRT1 in hepatocarcinogenesis, we conducted functional enrichment analyses using the Gene Ontology (GO) databases in proteomics and acetylome results mentioned above. The targets of SIRT1 were significantly enriched in RNA secondary structure unwinding, cytoplasmic translation, mRNA export, mRNA processing, translational initiation, and alternative mRNA splicing, all of which were closely related to RNA m^6A processing (Figure 2A).

We therefore focused on the regulatory factors related to m^{6}A modification obtained from volcano plots, and the considerable inhibition of FTO (0.659-fold enrichment in comparison to the control sample, $P < 0.001$) occurred following SIRT1 overexpression in proteome analysis. These results led us to consider FTO as the most obviously varied m^{6}A regulatory gene (Figure 2B and Supplemental Table 4). Western blotting of FTO had also the most significant change in both FTO-Hep3B and shFTO-HepG2 cells compared to other m^{6}A markers (Figure 2C). We also checked the immunofluorescence intensity and localization of FTO with the varied SIRT1 activity. The SIRT1 agonist SRT2104 and antagonist Selisistat were then introduced to HCC cell lines to regulate SIRT1 deacetylase activity. The optimal concentration of SRT2104 and Selisistat were 8 μM and 16 μM respectively (Supplemental Figure 2A). FTO was found to be negatively regulated by SIRT1, and it was mainly retained in nuclei (Supplemental Figure 2B).

Assuming a major contribution of SIRT1 to FTO inhibition and m^{6}A patterns, we next reasoned the magnitude of FTO in SIRT1-mediated HCC phenotypes *in vitro*. The gain/loss-of-function studies in terms of SIRT1 and FTO interfering experiments were conducted. SIRT1 promoted proliferation and invasion while inhibit apoptosis of Hep3B cells, whose effects were opposite to FTO. Importantly, co-transfection of both plasmids results in retarded oncogenic patterns, revealing that FTO largely counteracted the promoting role of SIRT1 in HCC tumorigenicity. HepG2 cells with sh-SIRT1 showed significantly tardy proliferating rate, higher apoptosis, and reduced invasive ability. The above changes were also reversed by FTO knockdown to a great extend (Figure 2D, 2E, 2F). Additionally, the decrease of FTO protein levels were detected in HCC samples compared to adjacent non-tumor tissues (Supplemental Figure 2C). These provide substantial evidence that FTO functions as tumor suppressor in HCC tumorigenesis.

To initially decipher the mechanisms on how SIRT1 downregulates FTO, PCR test was performed showing that the mRNA level of FTO was not affected by SIRT1 (Supplemental Figure 2D). We then explored whether FTO was downregulated by SIRT1 via its deacetylase property. The very faint bands made it evident that no acetylating modification of FTO or SIRT1-FTO protein interaction were detected in co-immunoprecipitation experiments (Supplemental Figure 2E). These data were in line with our acetylating array that no predicted acetylating sites in FTO were detected. In another way, FTO has a markedly inhibitory effect on HCC growth, and its downregulation is indispensable for SIRT1-mediated hepatocarcinogenesis. The FTO, however, is not the direct transcriptional or deacetylating target of SIRT1.

SIRT1 enhances RANBP2 stability through its deacetylating property

The Hypotheses regarding FTO protein instability affected by intermediates came to light under changings of multiple substrates of SIRT1 from the above screening microarrays and bioinformatic approaches. The GO analysis in our protein and acetylation arrays collectively pointed to the biological process termed protein SUMOylation (Figure 2A). Certain SUMO molecules were induced by SIRT1, and this effect was most notable in multiple sites of E3 SUMO-protein ligase RANBP2 (Figure 3A and Supplemental Table 5). In accordance with proteome and acetylome results, SIRT1 markedly reduced RANBP2 acetylation level as well as increased protein level (Figure 3B). Co-immunoprecipitation and co-localization assays additionally proved that both exogenous and endogenous SIRT1 interacted with RANBP2 in the nucleus (Figure 3C and 3D). The cycloheximide (CHX)-based protein stability assay was conducted since acetylation has long been verified to affect protein functions through diverse mechanisms including by regulating protein stability and enzymatic activity (22). RANBP2 protein expression was enhanced when treated with agonist SRT2014, and

conversely, the antagonist Selisistat effectively reduced RANBP2 expression. These initially proved that deacetylation facilitated RANBP2 protein stability (Figure 3E). We next investigated whether deacetylation affects RANBP2 protein degradation using both CHX and proteasome inhibitor MG132. The shrinking of RANBP2 protein expression induced by Selisistat was saved by MG132, confirming that the acetylation by Selisistat contributed to RANBP2 protein proteasome degradation (Figure 3F). These provide substantial evidence that RANBP2 is the direct target of SIRT1. Specifically, SIRT1 activates RANBP2 and increases its stability in regard to attenuating RANBP2 protein degradation via deacetylation property.

E3 SUMO ligases RANBP2 mediates SIRT1-associated FTO downregulation

RANBP2 is a large nucleoporin endowed with SUMO E3 ligase and act as specificity factors and enhancers in the modification process (23). We wondered whether SIRT1 drove FTO expression via the activated RANBP2. Immunoblotting with anti-SUMO2/3 and anti-ubiquitin antibody for immunoprecipitation complex with anti-FTO antibody showed that the activated SIRT1 appeared to have significant effect of FTO SUMOylation and ubiquitination. To be specific, Lysine 48 (K48), the ubiquitin-binding platform that directly links to proteasome, was also found to be enriched in the presence of agonist SRT2104. This finding indicated that FTO downregulation was largely dependent on SIRT1 protein activity. Notably, co-immunoprecipitation analyses showed closer RANBP2-FTO interplays in the presence of SRT2104, suggesting a structural interaction in addition to ubiquitination tagging (Figure 4A, schematic diagram shown in 4B). Next, we transfected si-RANBP2 into HCC cells, the depletion of RANBP2 retarded the FTO protein downregulation even under SIRT1 activation. The ubiquitination assays proved that FTO instability was due to RANBP2 since its absence were unable to continue the FTO decrease via K48-linked ubiquitination (Figure 4C).

Immunofluorescence staining displayed the higher FTO intensity following RANBP2 knockdown. Accordingly, we found that the activated SIRT1 did not decrease FTO intensity in depleted RANBP2 situation (Supplemental Figure 3). Protein stability assay was also conducted and such RANBP2-dependent FTO degradation was found in proteasomal pathway (Figure 4D). The above data identify RANBP2 as a decisive factor to the fate of FTO SUMOylation, ubiquitination, and instability.

SUMOylation at Lysine-216 site is crucial for SIRT1-dependent FTO degradation

As SUMOylation may affect interactions, stability, localization, and activity of targeted proteins, it is not easy to predict what aspects SUMOylation of FTO influences (24). Mutagenesis were next conducted to investigate whether SUMO in specific site resulted in FTO degradation. Bioinformatics analysis of FTO using GPS-SUMO tool identified six potential SUMO-conjugation sites, three of which were consensus motifs. The K216 and K34 residues were further screened as evolutionarily conserved SUMO consensus motifs, and K216 owned the relatively high probability score; The K422 sites, though not strictly conserved SUMO motif, also gained high score (Figure 5A and 5B). In the next step, we mutated the surface exposed SUMO-acceptor K216 and K422 as three forms respectively (K216R, K216H, K216S, K422R, K422H, K422S, sequencing alignments were shown in Supplemental Figure 4). By employing protein expression and total m^6A levels, vectors encompassing K216S and K422S were chosen as ideal tools since the substitution of the target K to S minimally affected FTO expression and its m^6A demethylase activity in comparison with FTO-WT (Figure 5C and 5D). It was consistent with FTO-SUMOylation event mediated by RANBP2 (previously shown in Figure 4B) that SUMO2/3 was readily immunoprecipitated with FTO-WT. Meanwhile, we also confirmed that SUMO2/3 bands of FTO-K216S detected by anti-FTO antibody were significantly

reduced compared with FTO-WT, demonstrating the selectivity of FTO-SUMO conjugation sites. Under these conditions, less ubiquitin-FTO and restorative FTO smears were also observed in SRT2104-treated K216S group. These results indicate that K216 mutation largely protects FTO from SUMOylation and degradation. In contrast to K216S, K422-mutation significantly decreased FTO-SUMO level while no delayed protein degradation was observed, suggesting the SUMOylating dynamic in K422 was not responsible for FTO degradation (Figure 5E). It is thus tempting to speculate that RANBP2 majorly targets FTO at K216 to promote FTO destabilization.

SIRT1 attenuates tumor suppressor GNAO1 mRNA expression in hepatocarcinogenesis through FTO-dependent m^{6}A modification

The anti-tumor effects of m^{6}A eraser FTO in HCC has been verified in our previous experiments, while SIRT1 may exerts its oncogenic property through degradation of FTO. This led us to speculate whether SIRT1 could affect mRNA and even protein levels of certain genes via improving their m^{6}A abundances in the case of downregulated FTO. The m^{6}A sequencing as well as RNA array amongst groups of control, SIRT1-overexpressing-, FTO-overexpressing, SIRT1- and FTO-overexpressing, were therefore conducted to get insights into transcriptional expression by m^{6}A-related fine regulation. Initially, genes having upregulated m^{6}A levels in SIRT1- overexpressing group compared to control group, downregulated m^{6}A levels in SIRT1- and FTO- overexpressing group compared to single SIRT1- overexpressing group, and downregulated m^{6}A levels in FTO overexpressing group in contrast to control group were sorted out since these were potential downstream targets subjected to SIRT1 in m^{6}A regulatory pattern. In parallel, the significantly differential transcripts abundance, either up- or down-regulated in terms of the corresponding levels from the similar group comparison, could be interpreted as the consequence of m^{6}A changing. We found the 29 genes with positive

m^{6}A-transcript correlation and 34 genes with negative one after drawing the Venn diagram (presented in Figure 6A). Considering the multiple differential RNA m^{6}A methylation sites that would generate diverse levels of transcripts, we excluded the 15 overlapped genes with both positive and inverse correlation of m^{6}A levels (in different regions) and expression of transcripts (if there were multiple). Then the 14 potential SIRT1-targetd genes with only positive correlation between m^{6}A and transcript expression might theoretically have function similar to "oncogenes", whereas 19 potential "tumor suppressors" were eligible for only negative association between m^{6}A and transcript (genes listed in Supplemental Table 6).

Nineteen selected "tumor suppressors" of interest were further evaluated from the aspects of clinical importance such as survival rates, differential expression, and other reported documents. Bioinformatic analysis was additionally performed to investigate the HCC suppressors as SIRT1-targeted candidates. GNAO1 was among the 11 overlapped genes whose significant downregulation was found in not only our proteomic results but also two HCC clinical datasets. Moreover, GNAO1 owned typicality and priority since it was also one of potential "tumor suppressors" in overlapping region of m^{6}A sequencing (Figure 6B). In view of multiple predicting m^{6}A binding sites in GNAO1 and the fact that SIRT1 attenuated GNAO1 through FTO, we next investigated whether GNAO1 was controlled by m^{6}A manner. The significantly incremental m^{6}A signals using total m^{6}A level analysis as well as m^{6}A dot blot were detected in the presence of SIRT1 in Hep3B cells, while FTO overexpression could largely block the m^{6}A promoting role of SIRT1. The similar effects of SIRT1 and FTO on m^{6}A modifications were also proved in HepG2 cells (Figure 6C). These results collectively suggest that SIRT1 would act as an HCC activator in FTO-dependent m^{6}A modification. MeRIP-qPCR analysis was then performed to delineate whether FTO targets GNAO1

mRNA. SIRT1 overexpression dramatically reduced the m^6A level of GNAO1 mRNA in Hep3B cells. Importantly, double transfection of SIRT1 and FTO showed almost the same hypo m^6A^+ level as the negative controls, suggesting that FTO attenuated the effects of SIRT1 in m^6A pathways. The gain or loss experiments in HepG2 cells further addressed the m^6A promoting and inhibiting roles of SIRT1 and FTO respectively (Figure 6D). In line with m^6A sequencing result, qPCR indicated that m^6A^+ GNAO1 level was negatively correlated with their corresponding mRNA expression (Figure 6E). The subtle regulation of GNAO1 mRNA expression was additionally confirmed by RNA stability assay that FTO-mediated m^6A erasing prominently augmented the half-life of GNAO1 mRNA and relieved its downregulation by SIRT1 (Figure 6F and Supplemental Figure 5A). Furthermore, western blotting and immunofluorescence jointly showed that SIRT1 resulted in the decreased FTO and GNAO1 expression as expected. Interestingly, the downregulation of GNAO1 by SIRT1 was reversed in the presence of an FTO (Supplemental Figure 5B, 5C, and 5D). Together, we firstly reveal the m^6A-related regulatory mechanism of GNAO1 via its mRNA stability.

GNAO1 was found to be downregulated in several HCC database, and lower expression of GNAO1 significantly correlated with poor disease-free survival of patients with HCC (Figure 7A and 7B). We next confirmed that depleted GNAO1 significantly enhanced HCC proliferation and invasion *in vitro* (Figure 7C, 7D, and 7E). Furthermore, correlation analysis result was indicative of the positive crosstalk between GNAO1 and FTO in HCC dataset (Figure 7F), while GNAO1 negatively correlated with Alpha Fetoprotein (AFP) expression (Supplemental Figure 6). GNAO1 is firstly revealed as one of downstream targets of FTO in SIRT1-dependent manner and tumor suppressor in HCC.

FTO has inhibitory effect on SIRT1-mediated *in vivo* hepatocarcinogenesis

Subcutaneous sarcoma models were employed as an extended effort to verify the proposed molecular basis of FTO involvement in SIRT1-abundant HCC samples. Overexpression of FTO compensated the tumorigenic ability of Hep3B cells in the presence of SIRT1 overexpression, while FTO knockdown largely counteracted the inhibiting role of SIRT1 silencing in HepG2 cells (Figure 8A). The tumorigenic capacities were determined based on the proliferation marker Ki-67 and apoptosis marker Caspase-3, using immunohistochemistry, in which SIRT1 and FTO expression was altered (Figure 8B). The expressing tendencies of GNAO1 as well as RANBP2 acetylation and FTO degradation were consistent with the previous *in vitro* results (Figure 8C and Supplemental Figure 7). These, along with the *in vitro* data, collectively indicate that SIRT1 is potentially involved in m^6A RNA modification via downregulating FTO in HCC tumorigenesis (Figure 8D).

Discussion

Our findings identify a novel m^6A modification role of RNA demethylase FTO degradation exerted by SIRT1. The significantly downregulated expression of FTO is observed in SIRT-overexpressing HCC cell lines, but it is not entirely due to its direct deacetylase targets of SIRT1. These feasible interactions are unlike PGC-1α or other downstream effectors directly attached to SIRT1 in HCC (25, 26). With regards to the hypothesis of SUMOylation model underlying FTO downregulation by SIRT1 in HCC, we investigate the potential role of RANBP2 that is commonly involved in ubiquitin-like SUMO. The present study shows that FTO enables the greater precipitation of RANBP2 in the presence of abundant or activated SIRT1. RANBP2-depleted cells displayed the sustained higher expression of FTO despite under SIRT1 overexpression or activation, intensifying the structural model of endogenous RANBP2-FTO interaction.

The acetylation process dysregulated in HCC is unclear so far. This is the first study to illustrate the SUMO-related proteins as substrates affected by SIRT1. Our observation of the striking increase of RANBP2 by deacetylase SIRT1 provides compelling evidence supporting the model that site-specific acetylation within this basic interface is a central mechanism for the control of SUMO-mediated interactions. Attachment of the SUMO modifier to proteins occurs under noncovalent binding to SUMO-interaction motifs (SIMs) with negatively charged residues. Acetyl-mediated neutralization on SUMO frequently prevents its binding to SIMs and attenuates SUMO-mediated gene silencing, while deacetylation restores their catalytic function (23). SUMO acetylation controlled by class I/II Histone deacetylases (HDACs) is well established for decades, while recent biochemical experiments further uncover that SIRT1 favors SUMO2 chain formation as the K11 deacetylase (27). Intriguingly, as one of crucial nucleoporin, deacetylated RANBP2 may have profound effects on nucleocytoplasmic shuttling of substrates not limited to FTO, and this phenomenon was in consistence with the substrates subcellular localization subjected to acetylation (22). The site-specific deacetylation of E3 ligase RANBP2 by SIRT1 may indicate an intricate crosstalk between the SUMO system and signaling exerted by the protein deacetylase SIRT1 in the nucleus.

SUMO-related ubiquitination followed by targeted protein proteasome-associated degradation emerges as a common scene, and their interplay networks may be partly due to the given lysine sites (28). Here we find K216 as the overlapping site for both FTO ubiquitination and SUMOylation. Endogenous FTO is recently reported to undergo post-translational ubiquitination on the evolutionarily conserved K216 residue, and ubiquitin-deficient K216R mutation displays a slower FTO turnover in HeLa cells (29). Similarly, the potential SUMOylation sites are highly conserved among orthologues in different species, among which K216 is predicted as crucial SUMOylation site

in FTO modified by SUMO2/3. It has led to the idea that RANBP2-dependent K216-SUMOylation is necessary for FTO ubiquitination and even translocation, and the ongoing experiments in regard to interplays among various PTMs are expected to detail how SIRT1 facilitates FTO SUMOylation at multiple sites. It is worth noting that SUMO and ubiquitin E3-ligase has been also found in HCC tumorigenesis. The predicted K422 SUMO site of FTO, though not evolutionarily conserved SUMO consensus motifs located in C-terminal domain (CTD) or not directly responsible for FTO protein instability, is still an intriguing direction to supplement the fine-tuning of SUMO proteins extensively targeting FTO (30).

RNAs imply hundreds of distinct modifications at various sites. Due to the complexity of RNA structure and function, deciphering the biological roles of m^6A RNA modification, the most prevalent one for human mRNA, remains challenging although the m^6A binding sites are being consecutively predicted. While we have focused epi-transcriptomic and epi-genetic silencing function of FTO on tumor suppressor genes in HCC, other findings of m^6A functions in diverse carcinomas may sometimes be controversial because m^6A-modified genes vary substantially among different cell types and cancer status. A few studies characterized the deregulation of m^6A writers and erasers and their downstream targets. ALKHB5, an m^6A eraser, promotes breast cancer stem cell reprogramming and renewal by facilitating the removal of m^6A from NANOG mRNA and subsequent enhancing NANOG mRNA stability (21). As the m^6A erasers, FTO and ALKHB5 are reported to act as oncogenic and suppressing role in carcinogenesis respectively. More intriguingly, both m^6A writers METTL3 (31) and METTL14 (20) perform distinct role in HCC tumorigenesis. These findings indicate that not homologous function of carcinogenesis could be generalized by simplified m^6A modification machinery. In spite of previous finding that the slightly upregulated GNAO1 mRNA is detected in

midbrain and striatum of FTO-deficient mice, the ensemble of our data adds the FTO-mediated m^{6}A modification in epigenetic silencing of GNAO1 in HCC (32). With respect to specific downstream targeting genes, however, the same m^{6}A epi-transcriptomic changes seem not to necessarily attribute to similar trend towards the corresponding mRNA expression.

The identified m^{6}A binding sequence might be the decisive factors of mRNA expression following m^{6}A fine-tunings. Moreover, FTO protein mainly resides in the nucleus and partially co-localizes with nuclear speckles, indicating a dynamic model of m^{6}A demethylation at the level of mRNA stability via pre-mRNA processing (15). Besides, FTO is also found in the cytoplasm in several cell types, suggesting its potential role in modulating cytosolic mRNA expression (33, 34). Recent study involving RNA interactome prove that FTO does not interact with mature mRNA (35). Despite these controversies, FTO may govern more than one step in m^{6}A-dependent regulation.

HCC is fundamentally manifested with alterations in proteins that support tumor growth (36). GNAO1, whose deregulation previously found in epileptic encephalopathy and movement disorder, is firstly screened and validated to be HCC suppressor genes by our group (37). The depletion of FTO or other m^{6}A erasers is generally believed to result in the production of more abundant mRNA copies and expression of target proteins, but the actual effect on the expression of m^{6}A target proteins has been a long-standing puzzle in the field (38). We performed proteomic analysis, gain/loss-of-function studies both *in vitro* and *in vivo* to clarify that GNAO1 is downregulated predominantly via depleted FTO. This is consistent with a recent report that the demethylation of mRNA transcripts by FTO directly induces exon including phenotype (35). Apart from GNAO1, the potential downstream targets from our m^{6}A sequencing, either identified as “oncogenes” or “tumor suppressors”, are large repertoires of HCC treatment that need to be further elucidated.

The networks of SIRT1-mediated acetylation, SUMOylation, ubiquitination, and m^6A RNA modification in HCC tumorigenesis are presented step by step. Nevertheless, we are only the beginning to provide a basis for atypical RNA modifications regulated by SIRT1 that favors HCC progression. Based on these findings, a highly promising area of research would be the potential diagnostic biomarkers of SIRT1, RANBP2, FTO, and GNAO1. In addition, a better understanding of the complex networks of epitranscriptomic and epigenetic regulations in which SIRT1 is involved could reveal novel therapeutic strategies for HCC patients.

Authors contributions

XML and KC designed the study, analyzed and interpreted the data, and wrote the manuscript. JYL, WX and QHZ contributed to data acquisition, analysis and interpretation. HB performed all bioinformatics analysis. YXZ, LG, DH, XWX and FG carried out the experiments. RHL, MZ, WX, YHZ, JDZ, and XHL provide technical expertise and support. CXX, XC, XYW, FW, and QW provided clinical database compilation and analysis. All authors have seen and approved the final version of the manuscript.

Acknowledgments

We would like to thank Dr. Yung-Gui Yang (Chinese Academy of Sciences) and Dr. Pei-Jian He (Emory School of Medicine) for providing FTO plasmids and technical supports on the manuscript.

References

1. Cancer Genome Atlas Research Network. Electronic address wbe, Cancer Genome Atlas Research N. Comprehensive and Integrative Genomic Characterization of Hepatocellular Carcinoma. Cell 2017;169:1327-1341 e1323.

2. Lee IC, Ho XY, George SE, Goh CW, Sundaram JR, Pang KKL, Luo W, et al. Oxidative stress promotes SIRT1 recruitment to the GADD34/PP1alpha complex to activate its deacetylase function. Cell Death Differ 2018;25:255-267.

3. Deota S, Chattopadhyay T, Ramachandran D, Armstrong E, Camacho B, Maniyadath B, Fulzele A, et al. Identification of a Tissue-Restricted Isoform of SIRT1 Defines a Regulatory Domain that Encodes Specificity. Cell Rep 2017;18:3069-3077.

4. Wen D, Peng Y, Lin F, Singh RK, Mahato RI. Micellar Delivery of miR-34a Modulator Rubone and Paclitaxel in Resistant Prostate Cancer. Cancer Res 2017;77:3244-3254.

5. Lucena-Cacace A, Otero-Albiol D, Jimenez-Garcia MP, Munoz-Galvan S, Carnero A. NAMPT Is a Potent Oncogene in Colon Cancer Progression that Modulates Cancer Stem Cell Properties and Resistance to Therapy through Sirt1 and PARP. Clin Cancer Res 2018;24:1202-1215.

6. Zhang W, Luo J, Yang F, Wang Y, Yin Y, Strom A, Gustafsson JA, et al. BRCA1 inhibits AR-mediated proliferation of breast cancer cells through the activation of SIRT1. Sci Rep 2016;6:22034.

7. Portmann S, Fahrner R, Lechleiter A, Keogh A, Overney S, Laemmle A, Mikami K, et al. Antitumor effect of SIRT1 inhibition in human HCC tumor models in vitro and in vivo. Mol Cancer Ther 2013;12:499-508.

8. Chen J, Zhang B, Wong N, Lo AW, To KF, Chan AW, Ng MH, et al. Sirtuin 1 is upregulated in a subset of hepatocellular carcinomas where it is essential for telomere maintenance and tumor cell growth. Cancer Res 2011;71:4138-4149.

9. Lu Y, Xu W, Ji J, Feng D, Sourbier C, Yang Y, Qu J, et al. Alternative splicing of the cell fate determinant Numb in hepatocellular carcinoma. Hepatology 2015;62:1122-1131.

10. Luo C, Cheng Y, Liu Y, Chen L, Liu L, Wei N, Xie Z, et al. SRSF2 Regulates Alternative Splicing to Drive Hepatocellular Carcinoma Development. Cancer Res 2017;77:1168-1178.

11. Yang Y, Hsu PJ, Chen YS, Yang YG. Dynamic transcriptomic m(6)A decoration: writers, erasers, readers and functions in RNA metabolism. Cell Res 2018;28:616-624.

12. Geula S, Moshitch-Moshkovitz S, Dominissini D, Mansour AA, Kol N, Salmon-Divon M, Hershkovitz V, et al. Stem cells. m6A mRNA methylation facilitates resolution of naive pluripotency toward differentiation. Science 2015;347:1002-1006.

13. Wang X, Lu Z, Gomez A, Hon GC, Yue Y, Han D, Fu Y, et al. N6-methyladenosine-dependent regulation of messenger RNA stability. Nature 2014;505:117-120.

14. Jia G, Fu Y, He C. Reversible RNA adenosine methylation in biological regulation. Trends Genet 2013;29:108-115.

15. Jia G, Fu Y, Zhao X, Dai Q, Zheng G, Yang Y, Yi C, et al. N6-methyladenosine in nuclear RNA is a major substrate of the obesity-associated FTO. Nat Chem Biol 2011;7:885-887.

16. Li Z, Weng H, Su R, Weng X, Zuo Z, Li C, Huang H, et al. FTO Plays an Oncogenic Role in Acute Myeloid Leukemia as a N(6)-Methyladenosine RNA Demethylase. Cancer Cell 2017;31:127-141.

17. Sigurdson AJ, Brenner AV, Roach JA, Goudeva L, Muller JA, Nerlich K, Reiners C, et al. Selected single-nucleotide polymorphisms in FOXE1, SERPINA5, FTO, EVPL, TICAM1 and SCARB1 are associated with papillary and follicular thyroid cancer risk: replication study in a German population. Carcinogenesis 2016;37:677-684.

18. Widagdo J, Chai YJ, Ridder MC, Chau YQ, Johnson RC, Sah P, Huganir RL, et al. Activity-Dependent Ubiquitination of GluA1 and GluA2 Regulates AMPA Receptor Intracellular Sorting and Degradation. Cell Rep 2015.

19. Huang H, Weng H, Sun W, Qin X, Shi H, Wu H, Zhao BS, et al. Recognition of RNA N(6)-methyladenosine by IGF2BP proteins enhances mRNA stability and translation. Nat Cell Biol 2018;20:285-295.

20. Ma JZ, Yang F, Zhou CC, Liu F, Yuan JH, Wang F, Wang TT, et al. METTL14 suppresses the metastatic potential of hepatocellular carcinoma by modulating N(6) -methyladenosine-dependent primary MicroRNA processing. Hepatology 2017;65:529-543.

21. Zhang C, Samanta D, Lu H, Bullen JW, Zhang H, Chen I, He X, et al. Hypoxia induces the breast cancer stem cell phenotype by HIF-dependent and ALKBH5-mediated m(6)A-demethylation of NANOG mRNA. Proc Natl Acad Sci U S A 2016;113:E2047-2056.

22. Narita T, Weinert BT, Choudhary C. Functions and mechanisms of non-histone protein acetylation. Nat Rev Mol Cell Biol 2018.

23. Ullmann R, Chien CD, Avantaggiati ML, Muller S. An acetylation switch regulates SUMO-dependent protein interaction networks. Mol Cell 2012;46:759-770.

24. Chen C, Zhu C, Huang J, Zhao X, Deng R, Zhang H, Dou J, et al. SUMOylation of TARBP2 regulates miRNA/siRNA efficiency. Nat Commun 2015;6:8899.

25. Mao B, Hu F, Cheng J, Wang P, Xu M, Yuan F, Meng S, et al. SIRT1 regulates YAP2-mediated cell proliferation and chemoresistance in hepatocellular carcinoma. Oncogene 2014;33:1468-1474.

26. Kleiger G, Mayor T. Perilous journey: a tour of the ubiquitin-proteasome system. Trends Cell Biol 2014;24:352-359.

27. Gartner A, Wagner K, Holper S, Kunz K, Rodriguez MS, Muller S. Acetylation of SUMO2 at lysine 11 favors the formation of non-canonical SUMO chains. EMBO Rep 2018;19.

28. Gibbs-Seymour I, Oka Y, Rajendra E, Weinert BT, Passmore LA, Patel KJ, Olsen JV, et al. Ubiquitin-SUMO circuitry controls activated fanconi anemia ID complex dosage in response to DNA damage. Mol Cell 2015;57:150-164.

29. Zhu T, Yong XLH, Xia D, Widagdo J, Anggono V. Ubiquitination Regulates the Proteasomal Degradation and Nuclear Translocation of the Fat Mass and Obesity-Associated (FTO) Protein. J Mol Biol 2018;430:363-371.

30. Li J, Xu Y, Long XD, Wang W, Jiao HK, Mei Z, Yin QQ, et al. Cbx4 governs HIF-1alpha to potentiate angiogenesis of hepatocellular carcinoma by its SUMO E3 ligase activity. Cancer Cell 2014;25:118-131.

31. Chen M, Wei L, Law CT, Tsang FH, Shen J, Cheng CL, Tsang LH, et al. RNA N6-methyladenosine methyltransferase-like 3 promotes liver cancer progression through YTHDF2-dependent posttranscriptional silencing of SOCS2. Hepatology 2018;67:2254-2270.

32. Hess ME, Hess S, Meyer KD, Verhagen LA, Koch L, Bronneke HS, Dietrich MO, et al. The fat mass and obesity associated gene (Fto) regulates activity of the dopaminergic midbrain circuitry. Nat Neurosci 2013;16:1042-1048.

33. Gulati P, Cheung MK, Antrobus R, Church CD, Harding HP, Tung YC, Rimmington D, et al. Role for the obesity-related FTO gene in the cellular sensing of amino acids. Proc Natl Acad Sci U S A 2013;110:2557-2562.

34. Yu J, Chen M, Huang H, Zhu J, Song H, Zhu J, Park J, et al. Dynamic m6A modification regulates local translation of mRNA in axons. Nucleic Acids Res 2018;46:1412-1423.

35. Bartosovic M, Molares HC, Gregorova P, Hrossova D, Kudla G, Vanacova S. N6-methyladenosine demethylase FTO targets pre-mRNAs and regulates alternative splicing and 3'-end processing. Nucleic Acids Res 2017;45:11356-11370.

36. Conigliaro A, Tripodi M, Parola M. SENP1 activity sustains cancer stem cell in hypoxic HCC. Gut 2017;66:2051-2052.

37. Pearson TS, Helbig I. Epileptic encephalopathy, movement disorder, and the yin and yang of GNAO1 function. Neurology 2017;89:754-755.

38. Xiao W, Adhikari S, Dahal U, Chen YS, Hao YJ, Sun BF, Sun HY, et al. Nuclear m(6)A Reader YTHDC1 Regulates mRNA Splicing. Mol Cell 2016;61:507-519.

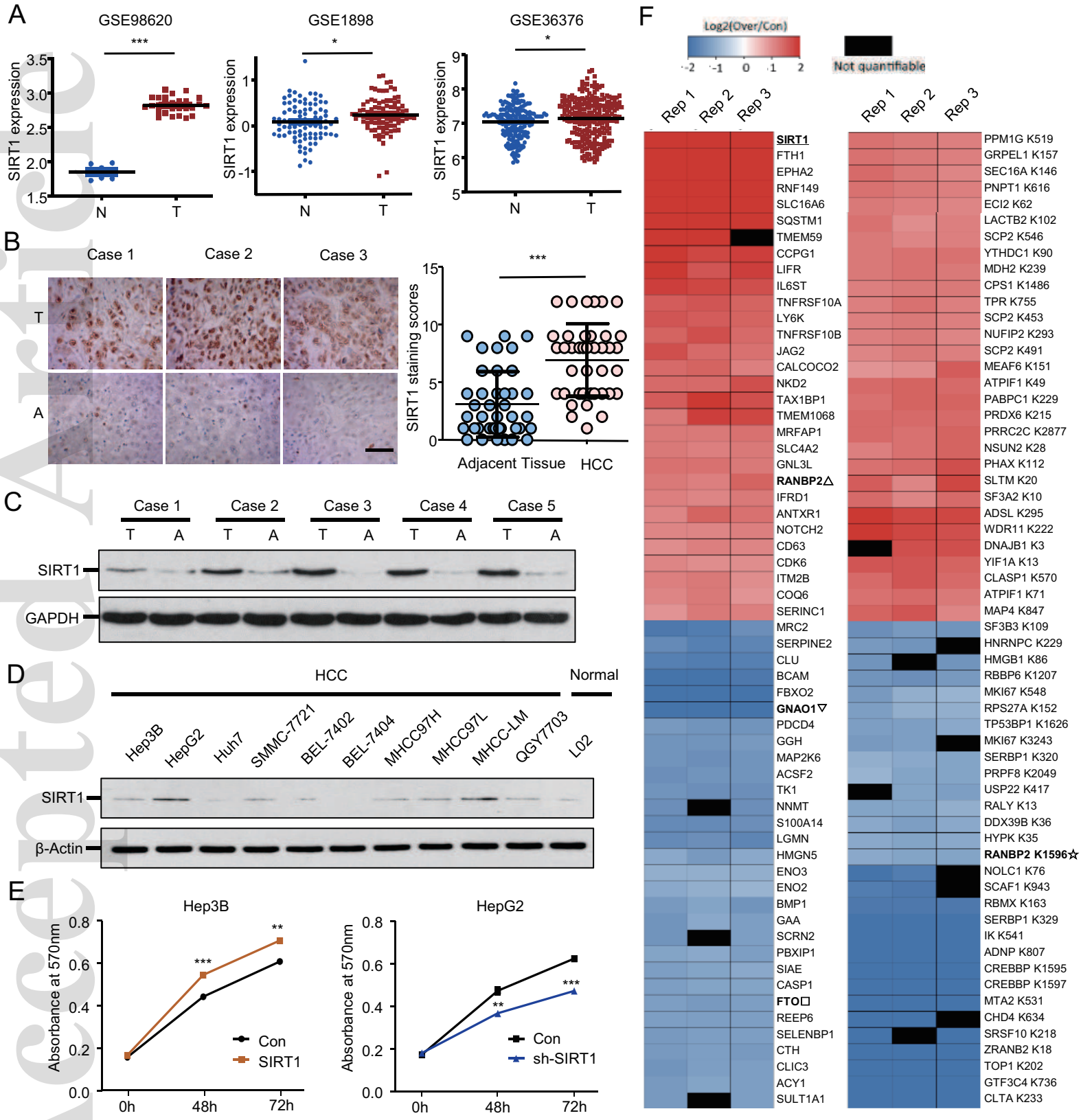

hep_31222_f1.eps

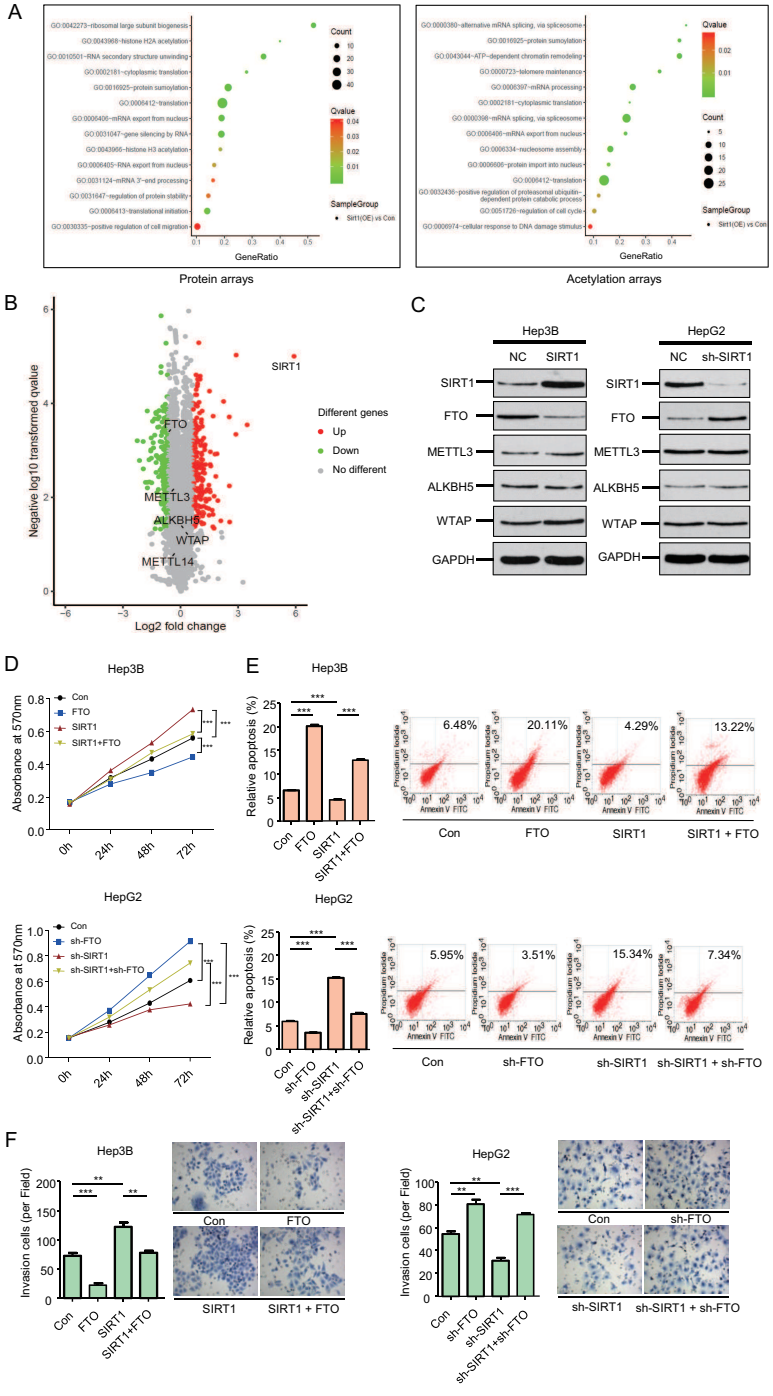

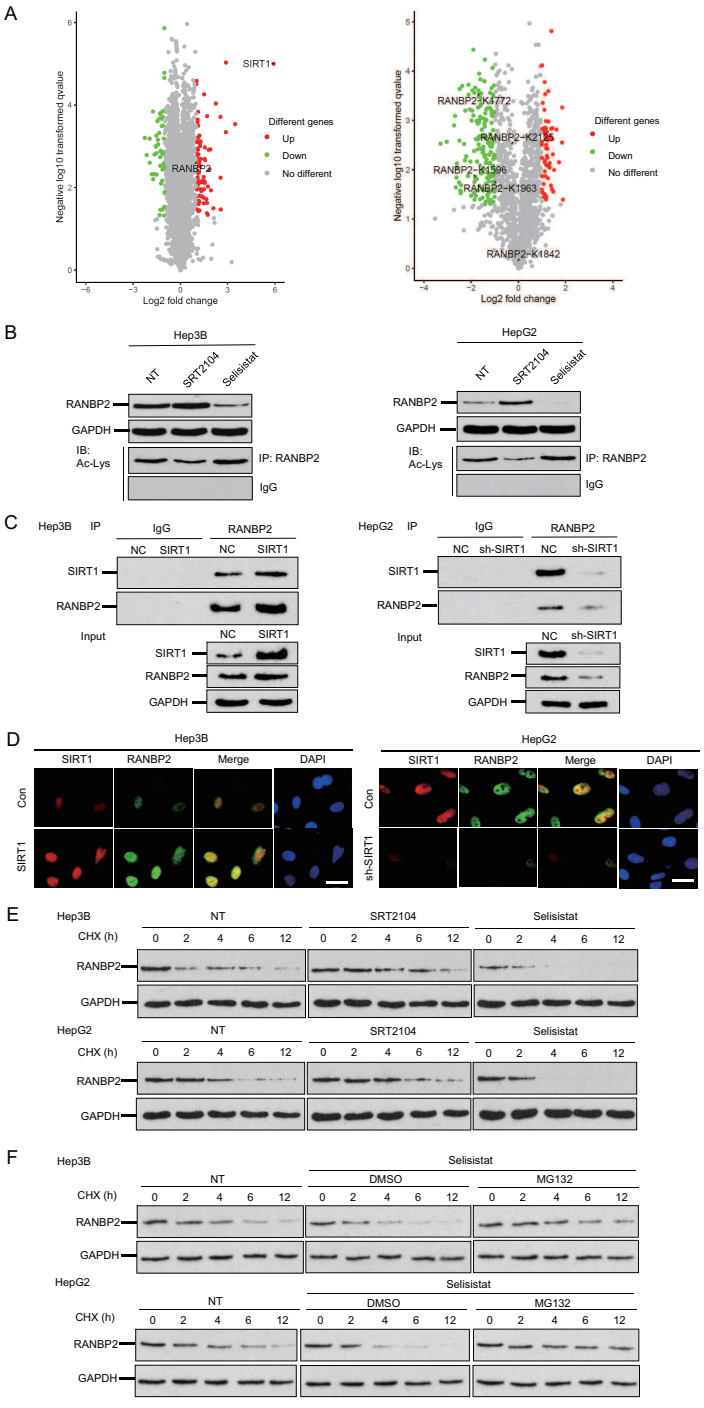

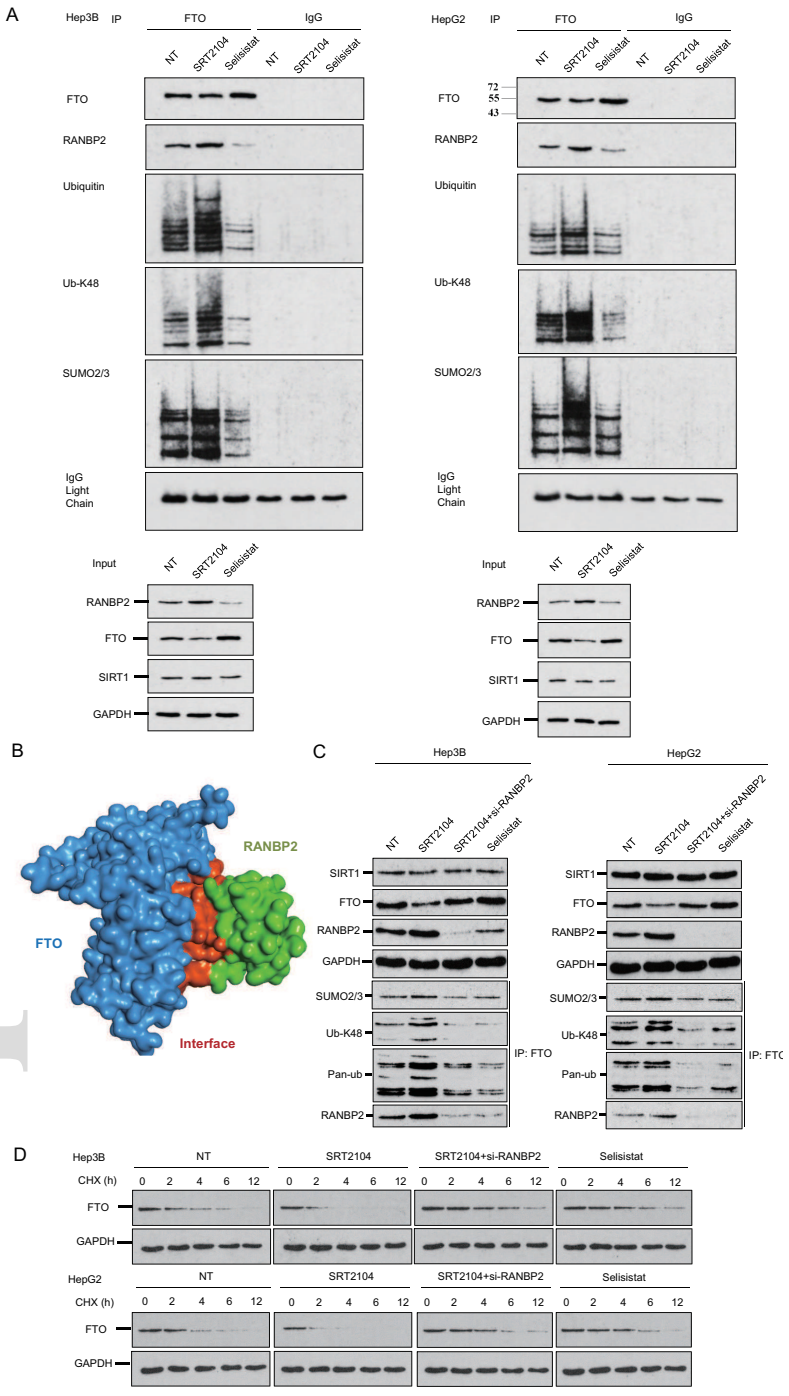

A

ID	Position	Peptide	Score	P-Value	Type
FTO	K34	WLPYLTP**K**DDEFYQQ	3.391	0.045	Sumoylation Concensus
FTO	K216	PQKMPYL**K**EEPYFGM	24.35	0.002	Sumoylation Concensus
FTO	K422	NAVLHEV**K**REGLPVE	20.264	0.002	Sumoylation Concensus
FTO	K469	RTLPADQ**K**PECRPYW	5.187	0.074	Sumoylation Nonconcensus
FTO	K478	ECRPYWE**K**DDASMPL	4.961	0.128	Sumoylation Nonconcensus
FTO	K504	RGQLLEA**K**P******	5.792	0.045	Sumoylation Nonconcensus

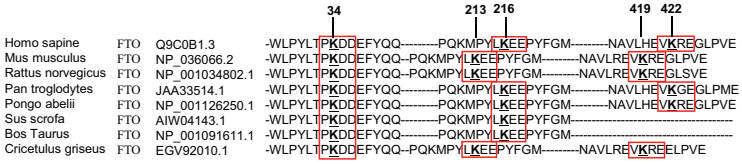

B

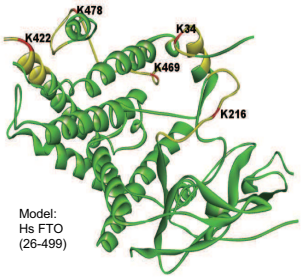

C

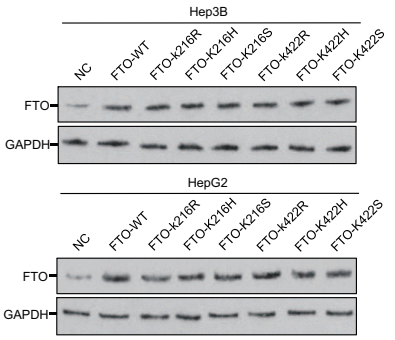

D

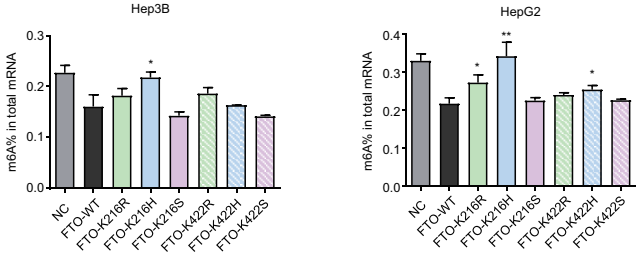

E